

Modeling and Simulation of Camera Positioning Stance on the Basis of Different Error Sources

Fan Chen¹, Ming Shang¹, Anjia Wang¹, Adiya Yadamsuren^{2,3} and Youqing Ma^{2,4,*}

¹Shenhua Shendong Coal Group Corporation, Ltd., Shanxi, China

²Key Laboratory of Digital Earth Science, Aerospace Information Research Institute, Chinese Academy of Sciences, Beijing, China

³Wild Camel Protection Foundation Mongolia, Ulaanbaatar, Mongolia

⁴International Research Center of Big Data for Sustainable Development Goals, Beijing, China

Received 1 September 2024; Accepted 29 October 2024

Abstract

High-definition (HD) cameras and Light Detection and Ranging (LiDAR) are used for foreign object identification and volume alarm provision on coal transport lines, and improving the accuracy of jointly calibrated HD camera and LiDAR data is essential. To determine the effect of errors on camera parameters through the classical image backward rendezvous model, this study proposed an evaluation model for the error sources in backward rendezvous. Positioning accuracy was analyzed by assuming the existence of systematic errors in camera principal distance and image principal point offset and the presence of random errors in the image point and LiDAR point cloud coordinates. The accuracy of the computational model was verified through experiments. Results demonstrate that, the positioning accuracies are $-23.2 \text{ mm} \pm 17.4 \text{ mm}$, $-20.6 \text{ mm} \pm 17.5 \text{ mm}$, and $-2.9 \text{ mm} \pm 19.6 \text{ mm}$ at a given random error of 0.02 m in the control point and at an error of 1 pixel in the image point. Increasing the control point improved the accuracy of camera positioning. The systematic errors in the camera's principal distance and in the image point coordinates affect the accuracy of positioning. This study provides a theoretical basis for the joint calibration of HD cameras and LiDAR, which is crucial for improving the accuracy of foreign object identification and volume alarm functions in coal transport lines.

Keywords: Camera positioning and staking, System error, Random error, Rear rendezvous, Joint calibration

1. Introduction

As one of the key means of spatial positioning and navigation, rear rendezvous technology is widely used in multisource joint calibration, precision engineering measurement, and deformation monitoring of large structures with high positioning accuracy and speed [1-3]. With the rapid development of modern science and technology, stringent requirements have been put forward for rear rendezvous technology, and research and development of high-performance rear rendezvous systems have become the focus of scholars at home and abroad. The traditional rear rendezvous system often ignores environmental factors and the influence of errors on the measurement process, and it is only suitable for applications with low accuracy requirements.

Rearward rendezvous, with its advantages of high performance, high accuracy, and robustness, has become a research hotspot because it can meet the demands of high performance and accuracy for specific occasions; it has been applied in multisource co-calibration, precision engineering measurement, and deformation monitoring of large-scale structures [1-3]. Research on rearward rendezvous technology has achieved substantial progress, but the complexity of the environment and the existence of measurement errors pose challenges to research on control

and error correction of rearward rendezvous systems.

On this basis, researchers have conducted many studies on the solution methods of backward rendezvous [4-7]. However, problems, such as the effect of the environment on positioning accuracy and insufficient error correction capability, still persist. Other existing algorithms consider the influence of environmental factors on positioning accuracy and improve the accuracy and reliability of positioning results through effective error correction strategies [8,9]. However, these methods are usually sensitive to the setting of the initial parameters, which affect the final calculation results and cannot meet the demand for fast positioning in practical application scenarios. Therefore, exploring other robust and efficient rear rendezvous algorithms remains to be an urgent task for current research.

On the basis of the analysis above, this study comprehensively explored the error sources of rear rendezvous technology by considering the actual needs of Baode Coal Processing Plant. The aim was to establish an accurate, efficient rear rendezvous evaluation model and determine the main factors that cause rear rendezvous errors through simulation experiments. This work is expected to provide powerful support for the intelligent acquisition of the underbody volume information of coal vehicles and for the realization of unmanned operation of the monitoring room of Baode Coal Processing Plant.

*E-mail address: mayq@radi.ac.cn

ISSN: 1791-2377 © 2024 School of Science, DUTH. All rights reserved.

doi:10.25103/jestr.175.23

2. State of the art

Researchers have conducted extensive work on image-based backward rendezvous. Guo Zhonglei et al. [4] proposed a spatial backward rendezvous method by adopting the Levenberg–Marquardt (LM) method for large-attitude-angle images and found that the LM method can overcome the problems of nonconvergence caused by errors in the iterative process and inappropriate initial values in the case of the pathological state of the normal-equation coefficient array; it reliably solves the outer orientation elements when the initial values of these elements of the image exhibit large deviation from the true values. However, the computational overhead is large and imposes certain requirements on computational resources. Wang Yongbo et al. [5] proposed a spatial backward rendezvous algorithm that is based on the unit quaternion description and the covariance equation. The unit quaternion was used to describe it, and matrix differentiation was adopted to differentiate the covariance equation. The similar transformation initial value problem caused by the linearization of the covariance equation is avoided, but the computational complexity of the algorithm increases when it deals with complex scenes. Jiatian Li et al. [6] proposed a supervised learning method for solving single-image-space backward rendezvous; they achieved a camera positioning accuracy that was higher than 4 m, but the model training requirement was high and required a large amount of labeled data and computational resources. Li Jiayuan et al. [7] developed a scale-adaptive Cauchy robust estimation model and improved the performance of the model by using an asymptotic optimization method. The model has a wide range of application prospects in the field of surveying and mapping and can effectively improve the accuracy and stability of data processing. In addition, the study verified the effectiveness of the model through examples, thus providing new ideas and methods for research in related fields. However, the model exhibits limitations in the presence of extreme outliers. Wang et al. [9] proposed a method to calculate the spatial backward rendezvous model on the basis of the random sample consensus algorithm. The method can accurately calculate the parameters of the spatial backward rendezvous model and improve the stability and accuracy of the calculation. Through theoretical analysis and experimental validation, the study proved the effectiveness and practicability of the method, which provides a new solution to related problems in photogrammetry. However, the computational efficiency of the method is affected when it deals with large datasets. Mustafa et al. [15] proposed a robust 3D angular posterior rendezvous model on the basis of the LM method. The method can accurately solve the angular backward rendezvous problem and improve the computational accuracy and stability of the model. The study verified the effectiveness and accuracy of the method through examples and provided a new technical means for solving the 3D angular backward rendezvous problem. However, the method is sensitive to the setting of the initial parameters, which affect the final calculation results.

The solution method for the rearward rendezvous problem is a popular research issue. Huang Xu et al. [10] proposed a direct solution method for the rearward rendezvous problem under a single responsive geometry condition. The solution method avoids the traditional method's complex iterative computation and improves computational efficiency and accuracy. The study proved the effectiveness and practicality of the solution method through theoretical analysis and experimental verification and

provided a new solution to related problems in remote sensing image processing. However, the method has limitations when dealing with complex scenes or noisy images. Fu et al. [11] synthesized various feature information and proposed an improved rear rendezvous method. The method makes full use of the feature information in the image and improves the accuracy and reliability of the rendezvous results. The study also verified the effectiveness of the method through examples, providing new ideas and methods for related problems in the field of surveying and mapping. However, the method consumes considerable computation time when it is used to process high-resolution images. Zhang et al. [12] comprehensively analyzed the condition number of pathological problems in photogrammetry and provided a theoretical basis for judging and resolving pathological problems. Through theoretical derivation and example analysis, the study revealed the relationship between the condition number and pathological problems and provided a new method of data processing and quality control in photogrammetry. However, the method needs some adjustments and optimization when it is applied to specific problems. Habib et al. [13] developed an autonomous spatial backward rendezvous method that is based on point and line representations of freeform controlled linear features. The method can accurately extract feature information from the image and achieve autonomous spatial backward rendezvous. The study proved the effectiveness and practicality of the method through theoretical analysis and experimental validation and provided a new technical means for automated, intelligent photogrammetry. However, the method has certain requirements on image quality and resolution at the feature extraction stage.

The promotion and application of rear rendezvous technology are lacking, and its main application area is industrial surveying. Ataiwe et al. [1] performed a comprehensive review and summary of spatial rear rendezvous problems in photogrammetry. The study determined the progress of research in this field and the problems involved, and it provided directions and ideas for future research. In addition, the study introduced the basic principles and methods of spatial backward rendezvous and offered an introductory guide for beginners. However, the review does not provide in-depth analyses of specific technical challenges and recent advances. Huang et al. [2] proposed a method based on industrial photogrammetry to address the problem of testing and evaluating the accuracy of aviation tires. The method can accurately measure the size and shape accuracy of tires and provides strong technical support for the quality control of tires. The study verified the effectiveness and accuracy of the method through examples, thus providing a new solution for research and application in related fields. However, the method can affect the accuracy of the measurement results when the tire surface has stains or severe wear. Zhang et al. [3] presented a new method to calibrate RGB-D cameras on the basis of 3D control fields. The method can accurately calibrate the internal and external parameters of these cameras and improve measurement accuracy. The study proved the effectiveness and accuracy of the method, which provides a strong technical guarantee for the application of RGB-D cameras, through theoretical analysis and experimental verification. However, the method requires a high-precision 3D control field in the calibration process, which may increase the complexity and cost of the experimental setup.

The joint calibration of LiDAR and cameras is one of the application scenarios of rear rendezvous. Omidalizarandi et al. [8] proposed a robust calibration method for the external calibration of terrestrial laser scanners and digital cameras. The method can accurately calibrate the relative positions and attitudes of the two sensors, thus providing accurate data support for structural monitoring. The study verified the validity and reliability of the method through examples and provided a new technical means for research and application in related fields. However, the method needs to closely and precisely measure the parameters in the calibration process to ensure the accuracy of the calibration results.

The abovementioned studies have achieved remarkable results on spatial backward rendezvous, but limitations still exist. First, they cannot meet the demand for joint calibration in the scenario of the current study. Second, the accuracy of attitude estimation and localization still needs to be improved. This study aims to achieve an accurate and robust spatial backward rendezvous model, analyze the sources of errors comprehensively, and present measures to avoid them. At present, the solution to the problem of intelligently acquiring attributed and geometric information on coal transport vehicles mainly relies on the use of devices, such as high-definition (HD) cameras and LiDAR, and adopts image and point cloud processing methods. The general steps include the alignment of images and point clouds, classification of foreign objects (segmentation and recognition of images and point clouds), and calculation of geometric information. To achieve high-precision alignment of HD camera and LiDAR data, this study investigated a vision-based method for high-precision camera position estimation and analyzed the accuracy and sources of error of this method. This research is crucial for realizing the unattended operation of the monitoring room of Baode Coal Processing Plant and the intelligent acquisition of coal transport vehicle information.

The remainder of the study is organized as follows. Section III describes the installation location and distribution of equipment and the construction of a model for rear rendezvous and error analysis. Section IV analyzes the image matching process through simulation experiments, the case where image points are uniformly distributed and contain random errors, and the case where image points are uniformly distributed and jointly affected by systematic and random errors. Section V summarizes the study and presents relevant conclusions.

3. Methodology

The distribution of cameras above the coal transport line is shown in Figure 1. Near the video surveillance room, a fixed bracket was installed. Digital cameras and LiDAR equipment were placed above the bracket to achieve accurate calculation of the volume of foreign objects in the vehicle compartment.

As shown in Figure 1, the HD digital camera arranged above the bracket and above the empty lane took pictures vertically downward to obtain images of the bottom of the vehicle. The LiDAR equipment derived point cloud information. Through image recognition technology, foreign objects (e.g., snow, red minerals, and debris) under the vehicle can be partially intelligently identified. Then, the volume of foreign objects in the foreign object area can be calculated from the LiDAR point cloud data. Therefore, the camera coordinate system must be unified with the LiDAR

coordinate system to achieve high-precision positioning and posturing of the camera (i.e., implement image rear rendezvous).

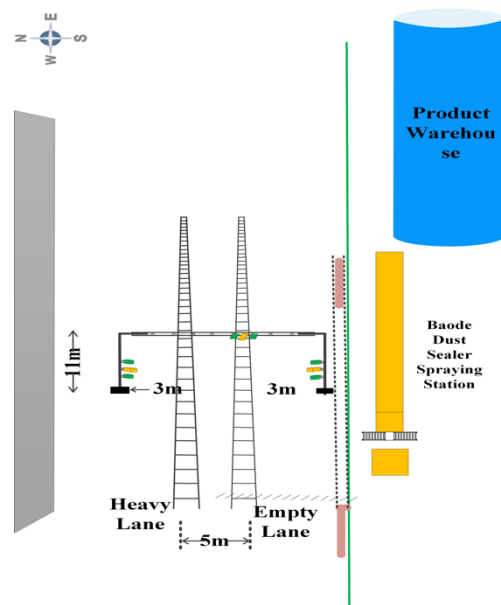


Fig. 1. Distribution of cameras over the coal route

Image rear rendezvous uses the beam leveling and positioning method, and the classical covariance equation [16] in photogrammetry is employed as the mathematical model. By adopting the plane coordinates of the control image points in LiDAR point cloud as observations, the position and attitude of the camera are determined as the parameters to be sought. After linearization of the nonlinear equations, with the attitude angle of the camera mounting position as the initial value, the optimal solution of the parameters to be sought is derived using a step-by-step iterative method. The positioning and attitude fixing results of the camera are then obtained. Compared with other visual positioning theories, the theory of the beam leveling method is more rigorous, and the stability of the positioning process and the accuracy of the positioning results are higher. The image back rendezvous model is shown in Figure 2.

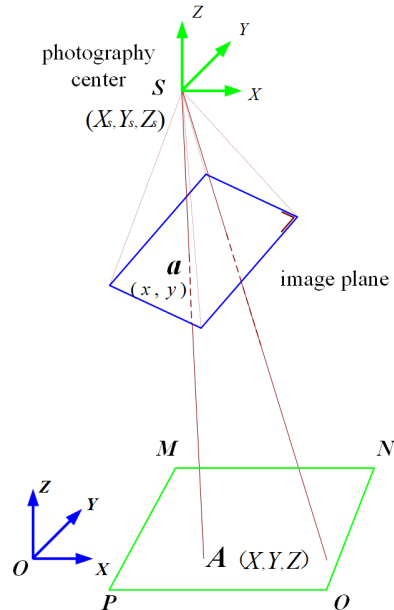


Fig. 2. Schematic of image back rendezvous

Assume that the image coverage is $MNPQ$, the coordinates of extracted feature point a in the image are (x, y) , and the 3D coordinates of the corresponding control point A are (X, Y, Z) . Moreover, assume that the camera position is (X_s, Y_s, Z_s) , and its three-direction attitude angle corresponding to the rotation matrix is R . Then, after combining the 3D coordinates of the control point and the coordinates of the image point, the covariance conditional equations can be established as:

$$\begin{aligned} x &= -f \frac{a_1(X - X_s) + b_1(Y - Y_s) + c_1(Z - Z_s)}{a_3(X - X_s) + b_3(Y - Y_s) + c_3(Z - Z_s)} \\ y &= -f \frac{a_2(X - X_s) + b_2(Y - Y_s) + c_2(Z - Z_s)}{a_3(X - X_s) + b_3(Y - Y_s) + c_3(Z - Z_s)} \end{aligned} \quad (1)$$

where f is the camera principal distance,

$$R^{-1} = \begin{bmatrix} a_1 & b_1 & c_1 \\ a_2 & b_2 & c_2 \\ a_3 & b_3 & c_3 \end{bmatrix}, \text{ and } a_1 \dots c_3 \text{ refers to the quantities}$$

comprising the trigonometric functions of the camera attitude angles. Camera position and attitude are the quantities to be solved, and after the linearization of Eq. (2), the error equation can be expressed as:

$$\begin{aligned} v_x &= \frac{\partial x}{\partial \phi} \Delta \phi + \frac{\partial x}{\partial \omega} \Delta \omega + \frac{\partial x}{\partial \kappa} \Delta \kappa + \frac{\partial x}{\partial X_s} \Delta X_s + \frac{\partial x}{\partial Y_s} \Delta Y_s \\ &+ \frac{\partial x}{\partial Z_s} \Delta Z_s + x^0 - x \\ v_y &= \frac{\partial y}{\partial \phi} \Delta \phi + \frac{\partial y}{\partial \omega} \Delta \omega + \frac{\partial y}{\partial \kappa} \Delta \kappa + \frac{\partial y}{\partial X_s} \Delta X_s + \frac{\partial y}{\partial Y_s} \Delta Y_s \\ &+ \frac{\partial y}{\partial Z_s} \Delta Z_s + y^0 - y \end{aligned} \quad (2)$$

The matrix representation of the error equation is

$$V = At + Bx - L \quad (3)$$

where V is the number of corrections to the image point coordinate observations, t is the position and attitude parameters of the camera, A is the matrix of its coefficients, x is the spatial 3D coordinates of the point to be determined, B is the matrix of its coefficients, and L is the vector of image point coordinate observations [17]. The corresponding normal equation can be obtained from Eq. (3) as:

$$\begin{bmatrix} A^T A & A^T B \\ B^T A & B^T B \end{bmatrix} \begin{bmatrix} t \\ x \end{bmatrix} = \begin{bmatrix} A^T L \\ B^T L \end{bmatrix} \quad (4)$$

The camera's initial mounting attitude angle was used as the initial value in the abovementioned iteration, and least squares iteration [17] was performed in combination with Eq. (4) to achieve accurate calculation of the camera positional parameters. The vibration of the train on the railway track during actual operation can affect the mechanical structure and calibration parameters of the camera. The camera principal distance and image principal point offsets can be considered to contain systematic errors, and the image point

coordinates and 3D point cloud coordinates of LiDAR contain random errors [18]. Next, camera positioning and attitude accuracy were evaluated under different systematic and random errors. The camera principal distance f is 3,491.79 pixels, the principal point offsets (x_0, y_0) are -8.85 and -8.21 pixel, the resolution is $2,448 \times 2,048$, and the field of view is $40^\circ \times 32.5^\circ$. Radial distortion parameters k_1 and k_2 are -0.032354 and 0.296282 , respectively, and tangential distortion parameters p_1 and p_2 are -0.001810 and 0.000389 , respectively. The coordinates of the control points extracted from the LIDAR point cloud (X, Y, Z) contain a random error (3σ) of 0.02 m, whereas the corresponding image points contain a 1-pixel random error. The image point matching coordinates and the control point coordinates obey a normal distribution [19]. The camera was mounted at a height of approximately 9 m and performed imaging at a 5° orientation toward the direction of oncoming traffic. The point cloud of the high-speed train acquired by LiDAR is shown in Figure 3.

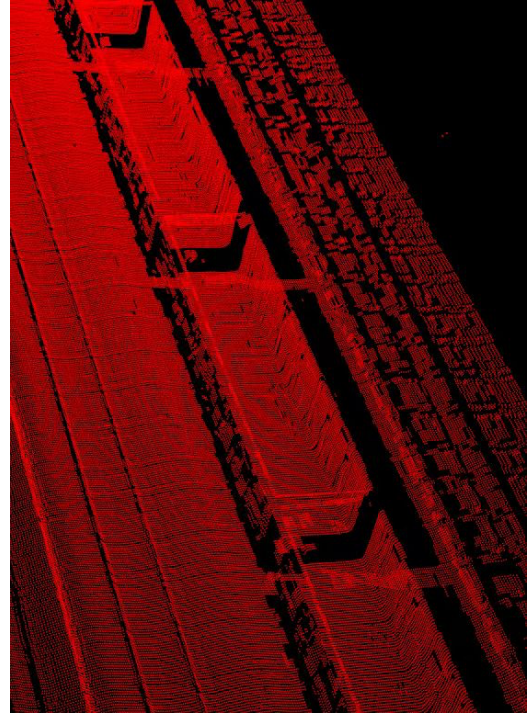


Fig. 3. High-speed train point cloud

3.1 Existence of systematic errors in camera principal distance

Assume that systematic error Δf exists in camera principal distance f . The computational model for camera positioning and fixing in the camera coverage is shown in Figures 4 and 5.

In Figures 4 and 5, S_1 is the camera exposure center, MN is the ground coverage, and A_1B_1 is the image plane. When the systematic error Δf is negative, the main distance of the camera decreases. $S_2A_2B_2$ needs to be translated and rotated at an angle to ensure that the imaging range is still MN . In the same process, when Δf is positive, the primary distance of the camera increases, and $S_2A_2B_2$ still needs to be translated and rotated.

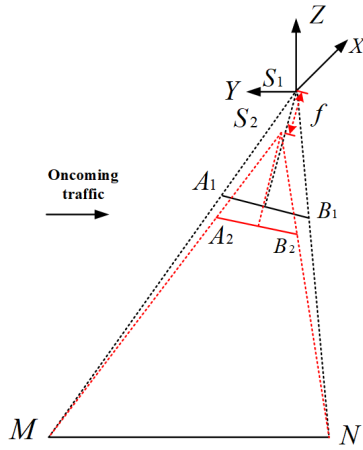


Fig. 4. Calculation model for camera positioning and fixing (the main distance has a systematic error; negative values, side view)

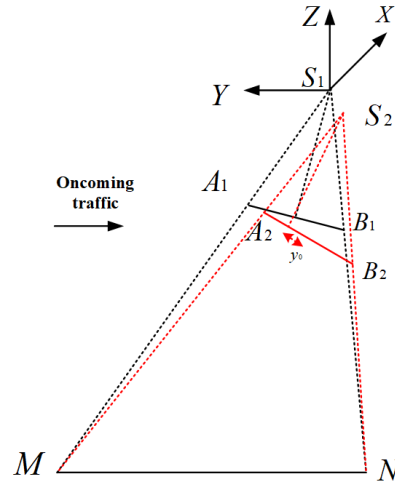


Fig. 6. Calculation model of camera positioning and fixing (main point y_0 has a systematic error; negative, side view)

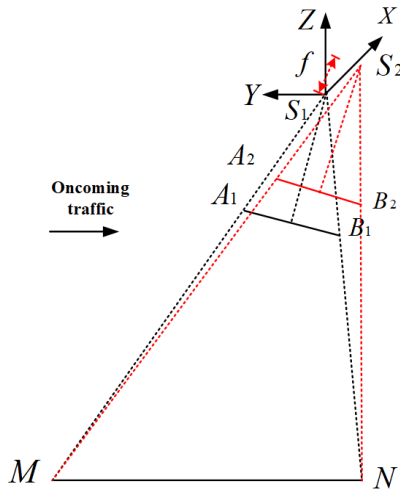


Fig. 5. Calculation model for camera positioning stance (the primary distance has a systematic error; positive values, side view)

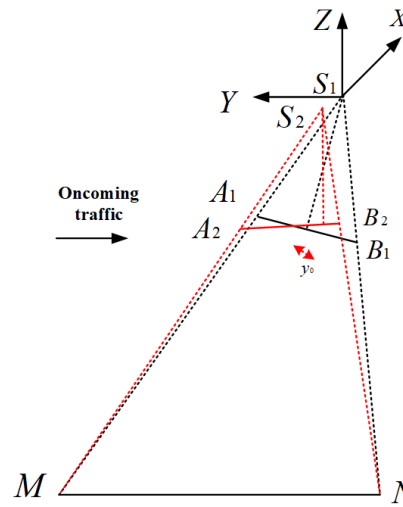


Fig. 7. Calculation model of camera positioning (main point y_0 has a systematic error; positive value, side view)

3.2 Existence of systematic errors in camera principal distance

Assume that the camera main point offsets (x_0, y_0) have systematic errors Δx_0 and Δy_0 . With camera main point offset y_0 as an example, the camera positioning stance calculation model within the camera coverage is shown in Figures 6 and 7.

As shown in Figures 6 and 7, when the systematic error at main point offset y_0 is negative, $S_2A_2B_2$ needs to be translated and rotated at an angle to ensure that the imaging range is still MN .

3.3 Consideration of image point matching and random errors in the control points

In Eq. (2), the feature-matched image point coordinates (x, y) are assumed to contain random errors ($3\sigma = 1$ pixel), and the control point 3D coordinates (X, Y, Z) contain random errors ($3\sigma = 0.02$ m), which affect the iterative solution of the camera's position and attitude parameters (t) . For this reason, the accuracy of camera positioning and attitude calculation needs to be verified under different combinations of random and systematic errors.

4. Result Analysis and Discussion

The camera position and attitude parameters (t) are assumed to be $0, -5^\circ$ (clockwise); $0, 0, 0, 9$ m; and true. The simulation combinations are as follows: (1) the image matching points are uniformly distributed and have a random error and (2) the image matching points are uniformly distributed and have systematic and random errors.

4.1 Experimental environment

The following experiments were performed 40,000 times in MATLAB R2017. The computer used had an Intel(R) Core(TM) i7-8750H CPU @ 2.20–2.21 GHz, with 16 G of memory.

4.2 Simulation experiment

4.2.1 Uniform distribution and random errors in image matching points

3D coordinates (X, Y, Z) of the control points were selected at equal intervals from the LiDAR point cloud within the coverage area $MNPQ$ in Figure 2. For the control point coordinates (X, Y, Z) containing a random error of 0.02 m, the corresponding image point contains a random error of 1 pixel, assuming that the lens distortion error is not

considered. The image point matching coordinates and the control point coordinates obey a normal distribution [20]. Table 1 shows the rear rendezvous accuracy under different numbers of control points.

Table 1. Camera positioning accuracy analysis

Mean value of differences/mm			Variance (statistics) (3σ)/mm				Quantities
X	Y	Z	X	Y	Z	XYZ	
-23.2	-20.6	-2.9	17.4	17.5	19.6	31.5	9
-23.1	-20.8	-3	17.4	17.5	19.7	31.6	4

Table 2. Camera positioning accuracy analysis

Mean value of differences/ $^\circ$			Variance (statistics)(3σ) $^\circ$			Quantities
φ	ω	κ	φ	ω	κ	
0.001818	-0.000664	0.007630	0.001715	0.001511	0.000936	9
0.002425	-0.00176	0.007633	0.001898	0.002139	0.000960	4

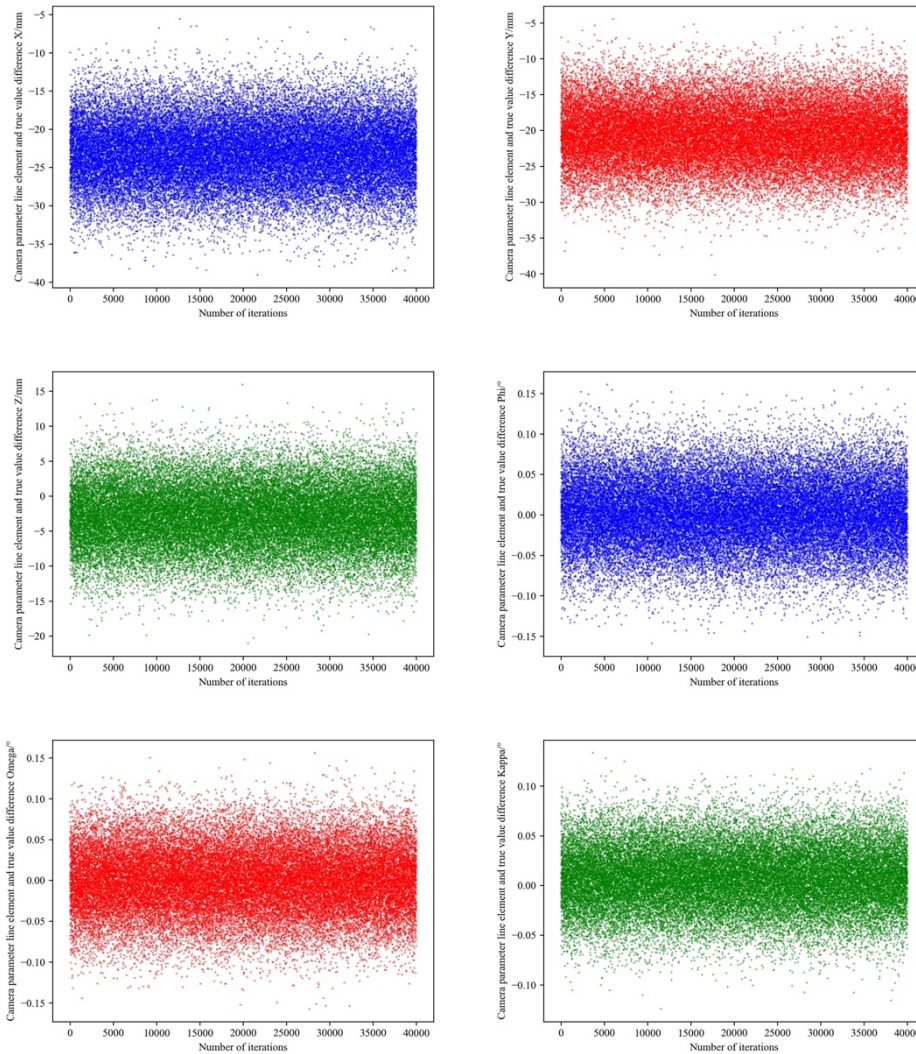


Fig. 8. Point distribution and accuracy analysis (uniform distribution of 9 points)

Comparison of Tables 1 and 2 shows that camera positioning accuracy increases with the increase in the number of control points. When the number of control points is 9, the accuracy of camera positioning (X_s, Y_s, Z_s) is -23.2 mm.

4.2.2 Uniform distribution of image matching points principal distance systematic error, and random error

The control point coordinates (X, Y, Z) still contain a random error of 0.02 m, and the corresponding image point contains

a random error of 1 pixel (assuming that the lens distortion error is not considered). The image point matching coordinates and the control point coordinates obey a normal distribution. Main distance f has a systematic error, and the values are set to $\pm 1\%f$, $\pm 2\%f$, and $\pm 5\%f$. The backward rendezvous accuracies under different numbers of control points are given in Table 3.

Table 3. Positioning accuracy analysis ($\pm 1\%$ systematic error in the main distance)

Mean value of differences/mm			Variance (statistics)(3σ)/mm				Quantities	f Systematic error
X	Y	Z	X	Y	Z	XYZ		
-23.1	-36.5	85.7	17.4	17.5	19.6	31.5	9	1%
-23.2	-36.1	85.8	17.4	17.50	19.6	31.5	4	1%
-23.1	-5.3	-91.7	17.3	17.4	19.5	31.3	9	-1%
-23.1	-5.3	-91.7	17.4	17.5	19.7	31.6	4	-1%

Table 4. Analysis of camera positioning accuracy ($\pm 1\%$ systematic error in the primary distance)

Mean value of differences/ $^{\circ}$			Variance (statistics) (3σ)/ $^{\circ}$			Quantities	f Systematic error
φ	ω	κ	φ	ω	κ		
0.001768	0.048979	0.007628	0.004315	0.002667	0.000987	9	1%
0.002410	0.047451	0.007629	0.005034	0.002682	0.001039	4	1%

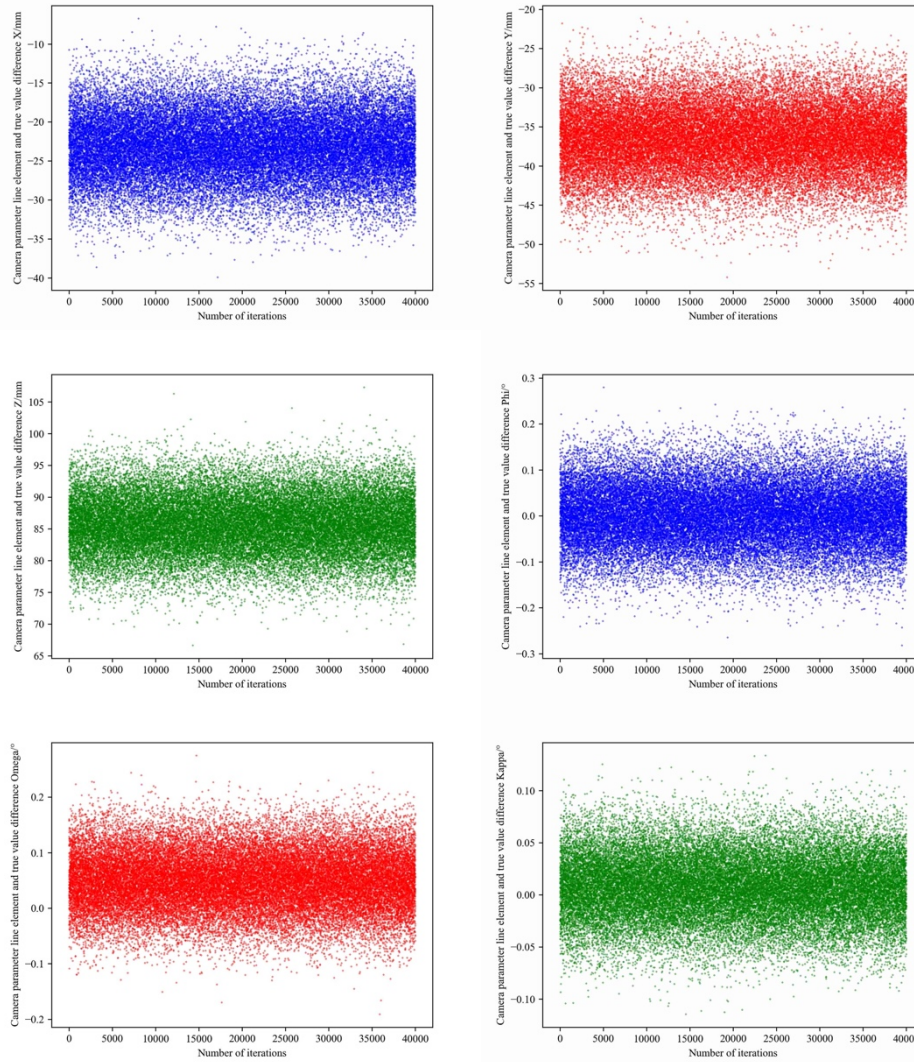


Fig. 9. Point distribution and accuracy analysis (9 points are uniformly distributed, with a systematic error of 1 pixel in the coordinates of the main point)

Figure 9 shows the distribution of camera positioning and fixing data in the case with 1% systematic error in the primary distance and 9 control points. Comparison of Tables 1, 2, 3, and 4 yields the following conclusions.

(1) According to Tables 3 and 4, with the increase in the number of control points, camera positioning accuracy increases. When the number of control points is 9, the accuracy of camera positioning (X_s, Y_s, Z_s) is $-23.1 \text{ mm} \pm 17.4 \text{ mm}$, $-36.5 \text{ mm} \pm 17.5 \text{ mm}$, and $85.7 \text{ mm} \pm 19.6 \text{ mm}$. The accuracy of the attitude angle in three directions is $0.001768^{\circ} \pm 0.004315^{\circ}$, $0.048979^{\circ} \pm 0.002667^{\circ}$, and $0.007628^{\circ} \pm 0.000987^{\circ}$.

(2) According to Tables 1 and 3, the main distance system error affects the calculated camera Z coordinates more than it affects the coordinates Y and Z mainly in terms of the mean value. The random error is nearly unanimous. This result indicates that the camera photographic center is displaced in the vertical direction to a large extent. This phenomenon is shown in Figures 4 and 5.

(3) According to Tables 2 and 4, the main distance system error considerably affects the calculation of the camera attitude angle mainly in terms of the mean value. The random error is also nearly unanimous. This finding indicates that the camera coordinate system has a large degree of rotation around the X axis, and the angular rotation

is not negligible. This phenomenon is shown in Figures 4 and 5.

(4) According to Tables 3 and 4, the main distance system error in the opposite direction affects the results of camera positioning and positioning calculation, which is mainly manifested by the phenomenon where the camera coordinate system rotates around the X axis in the opposite direction, and the angle is the same. The influence of the

systematic error of the main distance on the results of camera positioning and posing calculation was further verified. Table 5 shows the results of camera positioning and posing calculation when the systematic errors of main distance f are $\pm 2\%f$ and $\pm 5\%f$ and the number of control points is 9.

Table 5. Positioning accuracy analysis ($\pm 2\%f$ and $\pm 5\%f$ systematic errors in main distance)

Mean value of differences/mm			Variance (statistics)(3σ)/mm				Quantities	f Systematic error
X	Y	Z	X	Y	Z	XYZ		
-23	-52.2	174.4	17.5	17.5	19.7	31.6	9	2%
-23.1	10.1	-180.4	17.4	17.5	19.7	31.6	9	-2%
-23.10	-100.4	440.2	17.7	17.6	19.7	31.8	9	5%
-23.1	55.3	-446.8	17.40	17.40	19.6	31.5	9	-5%

Table 6. Analysis of camera positioning accuracy ($\pm 2\%f$ and $\pm 5\%f$ systematic errors in main distance)

Mean value of differences/ $^{\circ}$			Variance (statistics)(3σ)/ $^{\circ}$			Quantities	f Systematic error
φ	ω	κ	φ	ω	κ		
0.001738	0.098545	0.007628	0.007313	0.004545	0.001057	9	2%
0.001892	-0.1001657	0.007634	0.005620	0.004406	0.000917	9	-2%
0.001567	0.246783	0.007620	0.016711	0.010638	0.001384	9	5%
0.001989	-0.249916	0.007643	0.015035	0.010585	0.001074	9	-5%

From Tables 5 and 6, the following conclusions were obtained.

(1) The main distance system error affects the calculation of the camera Z coordinate more than it affects the calculation of coordinates Y and Z mainly in terms of the mean value. The random error is nearly the same.

(2) The main distance system error greatly affects the calculation of the camera attitude angle mainly in terms of the mean value, and the random error is nearly the same.

(3) Tables 5 and 6 indicate that the values of camera position Z and attitude angle are large, which verifies the accuracy of the modeling in Figures 4 and 5.

4.2.3 Image matching uniform distribution of image points and main point systematic and random errors

The control point coordinates (X, Y, Z) still contain a random error of 0.02 m, and the corresponding image point contains a random error of 1 pixel (assuming that the lens distortion error is not considered). The image point matching coordinates and the control point coordinates obey a normal distribution. A systematic error exists in the main point coordinates (x_0, y_0) , and the values are 1 and 5 pixels.

Table 7 shows the rear rendezvous accuracy under different systematic errors of the main point.

Table 7. Camera positioning accuracy analysis (1- and 5-pixel systematic errors exist in the main point coordinates)

Mean value of differences /mm			Variance (statistics)(3σ)/mm				Quantities	Coordinates of main point
X	Y	Z	X	Y	Z	XYZ		
-20.4	-18.2	-2.6	17.3	17.4	19.6	31.4	9	+1, +1
-25.7	-23.3	-3.3	17.4	17.5	19.7	31.5	9	-1, -1
-10	-8.1	-1.1	17.4	17.5	19.6	31.5	9	+5, +5
-36.1	-33.4	-4.8	17.4	17.5	19.6	31.5	9	-5, -5

Table 8. Camera positioning accuracy analysis

Mean value of differences/ $^{\circ}$			Variance (statistics)(3σ)/ $^{\circ}$			Quantities	Coordinates of the main point
φ	ω	κ	φ	ω	κ		
0.001608	-0.000521	0.006771	0.001513	0.001340	0.000917	9	+1, +1
0.002021	-0.000829	0.008495	0.001921	0.001694	0.000951	9	-1, -1
0.000789	0.000015	0.003323	0.000720	0.000644	0.000874	9	+5, +5
0.002839	-0.001528	0.011939	0.002724	0.002375	0.001037	9	-5, -5

Figure 10 shows the distribution of camera positioning fixing data in the case where a 1-pixel systematic error exists

in the coordinates of the main point and the number of control points is 9.

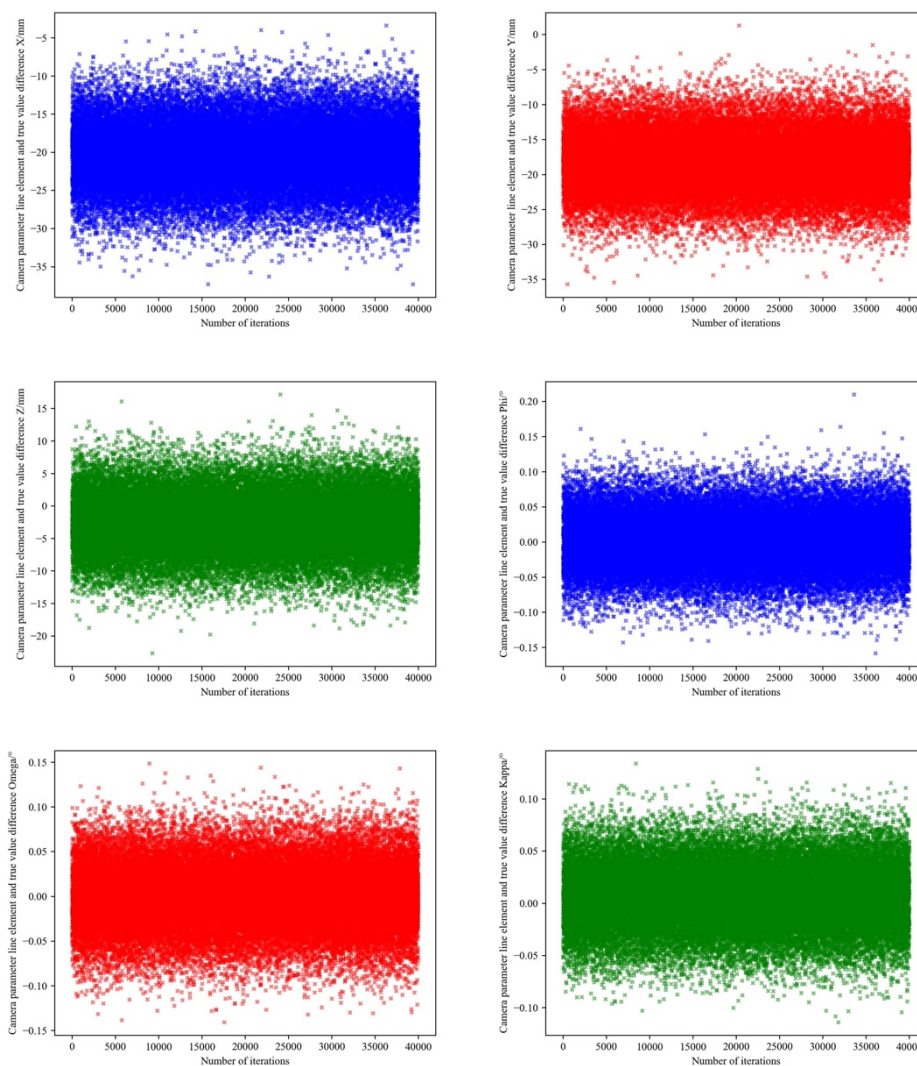


Fig. 10. Point distribution and accuracy analysis (9 points are uniformly distributed, with a systematic error of 1 pixel in the coordinates of the main point)

From Tables 7 and 8, the following conclusions were obtained.

(1) The main point system error considerably affects the calculation of camera coordinates X and Y , and the random error is nearly the same. This result indicates that the camera photographic center is substantially displaced in the image plane direction. This phenomenon is shown in Figures 6 and 7.

(2) The main point system error affects the accuracy of calculating the camera attitude angle, but the value is small. As the systematic error value of the offset of the main point of the image increases, the camera coordinate system rotates around the Y and Z axes, and the angular rotation is not negligible. This phenomenon was verified, as shown in Figures 6 and 7.

5. Conclusions

To achieve high-precision alignment of HD camera and LiDAR data, this study proposed a camera position estimation model that is based on different error sources. Assuming that the camera principal distance and image principal point offset contained systematic errors and that the image point coordinates and LiDAR 3D point cloud

coordinates contained random errors, this study evaluated camera positioning and calculated its accuracy under different systematic and random errors. The following conclusions were derived.

(1) When the image matching points are uniformly distributed and contain only random errors, camera positioning accuracy increases as the number of control points increases. When the number of control points is 9, the camera positioning (X_s, Y_s, Z_s) accuracies are $-23.2 \text{ mm} \pm 17.4 \text{ mm}$, $-20.6 \text{ mm} \pm 17.5 \text{ mm}$, and $-2.9 \text{ mm} \pm 19.6 \text{ mm}$, and the attitude angle accuracies in the three directions are $0.001818^\circ \pm 0.001715^\circ$, $0.000664^\circ \pm 0.001511^\circ$, $0.007630^\circ \pm 0.001730^\circ$, and $0.007630^\circ \pm 0.000936^\circ$.

(2) When the image matching points are uniformly distributed and the main distance has a systematic error, the systematic error in the main distance affects the calculation of the camera's Z coordinate more than it affects the calculation of coordinates Y and Z mainly in terms of the mean value. The random error is nearly unanimous. This result indicates that the camera photographic center is displaced in the vertical direction to a large extent. Meanwhile, the main distance system error affects the calculation of the camera attitude angle mainly in terms of the mean value, and the random error is nearly the same. This finding indicates that the degree of rotation of the camera coordinate system around the X axis is high, and this

angular rotation is not negligible. The main distance system error in the opposite direction affects the results of camera positioning and positioning calculation, which is mainly manifested by the phenomenon that the camera coordinate system rotates around the X axis in the opposite direction, and the angle is unchanged.

(3) When the image matching points are uniformly distributed and the main point coordinates have a systematic error, the main point systematic error considerably affects the calculation of camera coordinates X and Y , and the random error is nearly the same. This result indicates that the degree of displacement of the camera photographic center in the direction of the image plane is large; the main point systematic error affects the accuracy of calculating the camera attitude angle, but the value is small. As the systematic error value of the offset of the image principal point increases, the degree of rotation of the camera coordinate system around the Y and Z axes is high, and the angular rotation is not negligible.

This study combined theory and simulation, and the simulation experiment verified the influence of different error sources (systematic and random errors) on camera

positioning and staking accuracy. The accuracy of the camera positioning and staking calculation model was also verified. This work lays a theoretical foundation for the joint calibration of HD cameras and LIDAR equipment, but it still has some shortcomings. First, this study mainly relies on simulation experiments and lacks experimental verification in real scenarios, which may lead to a certain gap between theory and practical application. Second, although multiple error sources are considered, other error factors that have an important effect on positioning and fixing accuracy in practical applications may have been excluded in this study. Last, although this study explores the joint calibration of camera and LIDAR equipment, it does not provide an in-depth discussion of the specific joint calibration method and its implementation details. This important topic will be one of the directions of our future research.

This is an Open Access article distributed under the terms of the Creative Commons Attribution License.



References

- [1] T. N. Ataiwe, "Space resection in photogrammetry: A review," *Oil Gas Eng.*, vol. 2784, p. 050006, Jan. 2023. doi.org/10.1063/5.0140489.
- [2] G. Huang, W. Zhu, W. Wang, X. Xie, and H. Wang, "Test and evaluation of aviation die tyre accuracy based on industrial photogrammetry," *J. Beijing Inst. Technol.*, vol. 29, no. 3, pp. 393-398, Sep. 2020(in Chinese).
- [3] C. Zhang, T. Huang, and Q. Zhao, "A new model of RGB-D camera calibration based on 3D control field," *Sensors.*, vol. 19, no. 23, 2019, Art. no. 5082. doi:10.3390/s19235082.
- [4] Z. Guo, J. Zhai, and K. Deng, "Large attitude angle image space resection based on the LM method," *J. Wuhan Univ. (Inf. Sci. Ed.)*, vol. 41, no. 4, pp. 565-568, Jan. 2016(in Chinese).
- [5] Y. Wang, Y. Wang, and H. Yang, "Single-image space resection algorithm based on unit quaternion description," *J. China Univ. Min. Technol.*, vol. 44, no. 3, pp. 557-565, May. 2015(in Chinese).
- [6] J. Li, C. Jia, Y. Niu, X. A. Huai, P. Gao, and L. Yan, "A supervised learning method for solving single-image spatial backward rendezvous," *J. Wuhan Univ. (Inf. Sci. Ed.)*, vol. 44, no. 8, pp. 1144-1152, Aug. 2019.(in Chinese).
- [7] J. Li, Y. Zhang, M. Ai, and Q. Hu, "Scale-adaptive Cauchy robust estimation model for asymptotic optimisation and its applications," *J. Surv. Mapp.*, vol. 52, no. 1, pp. 61-70, Jan. 2023(in Chinese).
- [8] M. Omidalizarandi, B. Kargoll, J.-A. Paffenholz, and I. Neumann, "Robust external calibration of terrestrial laser scanner and digital camera for structural monitoring," *J. Appl. Geod.*, no. 2, pp. 105-134, Jun. 2019.
- [9] X. Liu and Z. Kang, "Space resection model calculation based on random sample consensus algorithm," in *SPIE Proceedings: 2nd ISPRS Int. Conf. Comput. Vis. Remote Sens. (CVRS 2015)*, Xiamen, FJ, China. 2016, p. 99010K.
- [10] X. Huang, Y. Zhang, J. Yang, L. Ma, X. Xiong, and R. Huang, "Direct solution of the posterior intersection under homography geometry," *J. Remote Sens.*, no. 3, pp. 431-440, May. 2016(in Chinese).
- [11] Z. Fu, F. Zhou, and Z. Yu, "Posterior intersection method integrating multiple features," *J. Surv. Mapp.*, vol. 43, no. 8, pp. 827-834, Aug. 2014(in Chinese).
- [12] Zhang Yongjun, Wu Lianfeng, and Lin Lu, "Conditional number index analysis of pathological problems in photogrammetry," *J. Wuhan Univ. (Inf. Sci. Ed.)*, vol. 35, no. 3, pp. 308-312, Mar. 2010(in Chinese).
- [13] A. Habib, H. T. Lin, and M. Morgan, "Autonomous space resection using Point- and Line-Based representation of FREE-FORM control Linear Features," *Photogramm. Rec.*, vol. 18, no. 103, pp. 244-258, Dec. 2010.
- [14] Y. T. Mustafa, "Vigorous 3D angular resection model using Levenberg-Marquardt method," *J. Surv. Geospat. Eng.*, vol. 1, no. 1, pp. 08-13, Mar. 2021.
- [15] D. J. Liu and B. Z. Tao, *Practical Measurement Data Processing Methods*, Beijing: Surv. Mapp. Press., pp. 79-81, 2000(in Chinese).
- [16] Y. Ma et al., "On-orbit high-precision visual localization and terrain reconstruction of Zhu Rong Mars rover," *J. China. Sci. Bull.*, vol. 67, no. 23, pp. 2790-2801, Dec. 2022(in Chinese).
- [17] Q. Hu, S. Ye, Z. Yu, and L. Huang, "Analysis of the impact of camera calibration parameters on the ranging accuracy of stereo vision," *J. Geomatics.*, vol. 48, no. 6, pp. 62-67, Jun. 2023(in Chinese).
- [18] Z. Huang, Y. Su, Q. Wang, and C. Zhang, "Research on calibration methods for extrinsic parameters of 2D LiDAR and visible light cameras," *J. China. Sci. Instrum.*, vol. 41, no. 9, pp. 121-129, Nov. 2020(in Chinese).
- [19] C. Sun, Y. Ma, G. Zhang, Y. Gao, and Q. Yu, "Calibration method for long-focus cameras based on affine approximate projection model," *J. Lasers.*, vol. 43, no. 4, pp. 93-103, Apr. 2023(in Chinese).
- [20] Y. Dai, Y. Ding, X. Feng, H. Wang, and Q. Wang, "Calibration method of LiDAR and visible camera based on EPnP algorithm," *Optoelectron. Technol.*, vol. 43, no. 2, pp. 166-172, Feb. 2023(in Chinese).